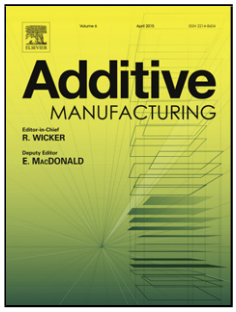

Title: 3-D printing of multifunctional carbon nanotube yarn reinforced components<!–<query id="Q1"> “Your article is registered as a regular item and is being processed for inclusion in a regular issue of the journal. If this is NOT correct and your article belongs to a Special Issue/Collection please contact a.arulanandaraj@elsevier.com immediately prior to returning your corrections.”</query>–>

Author: John M. Gardner Godfrey Sauti Jae-Woo Kim Roberto J. Cano Russell A. Wincheski Christopher J. Stelter Brian W. Grimsley Dennis C. Working Emilie J. Siochi

PII: S2214-8604(16)30127-0
DOI: http://dx.doi.org/doi:10.1016/j.addma.2016.06.008
Reference: ADDMA 106

To appear in:

Received date: 16-12-2015
Revised date: 21-4-2016
Accepted date: 6-6-2016

Please cite this article as: {http://dx.doi.org/

3-D Printing of Multifunctional Carbon Nanotube Yarn Reinforced Components

John M. Gardner[a], Godfrey Sauti[b], Jae-Woo Kim[b], Roberto J. Cano[a], Russell A. Wincheski[a], Christopher J. Stelter[a], Brian W. Grimsley[a], Dennis C. Working[a], Emilie J. Siochi[a]*

[a]NASA Langley Research Center, Hampton, VA 23681, USA
[b]National Institute of Aerospace, Hampton, VA 23666, USA

[*] Corresponding author: emilie.j.siochi@nasa.gov

Abstract

Continuous carbon nanotube (CNT) yarn filaments can be employed as an inherently multifunctional feedstock for additive manufacturing (AM). With this material, it becomes possible to use a single material to impart multiple functionalities in components and take advantage of the tailorability offered by fused filament fabrication (FFF) over conventional fabrication techniques. Some of the challenges associated with coupling this emerging material with advanced processing are addressed here through the fabrication and characterization of additively manufactured functional objects. Continuous CNT yarn reinforced Ultem® specimens are characterized to determine their mechanical and electrical properties. The potential to produce net shape fabricated multifunctional components is demonstrated by additively manufacturing a quadcopter frame using Ultem® and continuous CNT yarn reinforced Ultem®, where the CNT yarn reinforcement was designed to also act as the electrical conductors carrying current to the motors.

Keywords: carbon nanotube reinforced, 3D printing, multifunctional

1. Introduction

Carbon nanotubes (CNTs) are high aspect ratio nanoscale tubes whose atomic structure imparts a unique suite of mechanical, electrical and thermal characteristics [1] not usually possessed by a single material. Since their novelty was recognized over twenty years ago [2], this distinctive feature has led to visions of multifunctional materials and structures [3-6]. Early availability in powder form limited their utility to light doping of polymeric matrices to yield nanocomposites, thin films, and coatings with enhanced electrical properties sufficient for applications like electrostatic charge dissipation and electromagnetic shielding [7-10]. Until recently, the big payoff in multifunctional load bearing applications has been

challenging to attain due to the lack of bulk material formats that retain the attractive mechanical properties for which CNTs were heralded. The material is now available in commercial quantities of sheets and yarns [11] with mechanical properties that support their use as structural reinforcement [12-17], and electrical conductivity sufficient for data cables [18]. Spun yarns with good mechanical properties have also been shown to carry useful levels of current [19].

The advent of 3-D printing by fused deposition modeling (FDM) [20] or fused filament fabrication (FFF) permits the fabrication of geometrically complex parts inaccessible by conventional manufacturing techniques. Low cost, open-source 3D printers have provided easy access to a technique that can produce novel, topologically optimized functional components [21, 22]. Open-source machines typically use acrylonitrile butadiene styrene (ABS) and polylactic acid (PLA) feedstocks [23]. Higher performance filaments like Ultem® (polyetherimide) generally require more expensive FDM equipment due to the higher processing temperatures required. Feedstocks for multifunctional materials in AM have followed the initial trend in CNT nanocomposites using low volume fractions of dispersed CNTs. Filaments with low concentrations of graphene [24], graphene oxide [25] and metal particles [26] in a matrix have been studied. Conductive inks have also been used where conductive paths were desired [27-29]. Continuous carbon fiber, Kevlar® and glass fibers [30, 31] have been used to enhance part stiffness. The above set of feedstocks imparts only one functionality; therefore, a printer designed to combine the features offered by several of these materials in a part will require multiple print heads to accommodate different feedstock processing conditions. In contrast, CNTs offer the possibility of using a single material to tailor functionality with two print heads that can selectively lay down unreinforced and CNT reinforced elements in a part.

The coupling of FFF with continuous CNT yarn reinforced feedstock can change component design and fabrication paradigms by enabling net shape fabrication of multifunctional load bearing components, with the potential for cost effective manufacturing and performance enhancement. The work presented here demonstrates the advantages of using a single material to impart multiple functionalities to a net shape fabricated component. Parts made with the engineering polymer Ultem® were printed with portions continuously reinforced with CNT yarn and characterized to illustrate the following array of functions that can be embedded in an as-printed part: mechanical reinforcement, electrical conductivity, resistive heating and strain sensing. The integration of some of these functionalities in an article during fabrication is demonstrated by printing a quadcopter frame using Ultem® and continuous CNT yarn filament, where the CNT yarn functioned simultaneously as mechanical reinforcement and the electrical current carrying conductors.

2. Experimental Section

2.1 Filament preparation

Printable CNT yarn filaments consist of CNT yarn infused with Ultem®. They were fabricated by a scalable continuous solution coating method that enables wetting of the CNT yarn [15, 32]. A custom designed continuous coater was used for this process. As-received highly densified CNT yarn purchased from Nanocomp Technologies, Inc., Merrimack, NH ranged in specific strength and specific modulus from 1.33 to 1.59 N/tex, and from 69 to 102 N/tex, respectively, with linear densities of 24-29 g/km. The pristine CNT yarn was passed through a Teflon tube (3 mm in inner diameter), which contained a solution of 50 mg/ml Ultem® 1010 (Stratasys, Eden Prairie, MN) in dimethylacetamide (DMAc). The solution coated CNT yarn was heated to 250^{o}C to complete the filament preparation.

2.2 3D printing and cutting of continuous CNT yarn filament

A modified open-source, FFF 3D printer (Aleph Objects, Loveland, CO) was used to print components consisting of both neat Ultem® resin and CNT yarn filament by utilizing two separate nozzles heated to 375°C. Printing substrates were prepared by attaching an as-received 127 μm Ultem® sheet (McMaster-Carr, Robbinsville, NJ [33]) to the glass print bed with a high temperature adhesive (3M® 467MP). The substrate was cleaned with methanol prior to printing. The embedded electronic component sample was printed using a 3M® 8992 polyester film mounted in a similar fashion to the Ultem® substrate. Elmer's Disappearing Purple® glue stick was used as the substrate material in all other cases where neat Ultem® was printed prior to CNT yarn filament printing. The bed temperature during printing was maintained at 162°C. All other printing parameters developed in the course of this work are described in the Results and Discussion section.

The continuous CNT yarn filament was cut by resistive (Joule) heating. The section of CNT yarn filament to be cut was used to complete the circuit between the metallic print nozzle which contacts the filament as it is being extruded, and a second electrode located 3-5 mm below the nozzle. The spacing between the nozzle and second electrode ensured that a length of the filament suitable for starting the anchoring step in the next print run remained at the nozzle tip. A variable DC power supply (Rigol DP832 Programmable DC Power Supply) was used to cut the filament. To characterize the time response of the CNT yarn filament cutting, two Keithley 2000 Digital Multimeters (DMMs) were used to measure the voltage and current supplied by the DC power supply. Custom-built LabVIEW (National Instruments) based software was used for data acquisition from the DMMs.

2.3 Material and part characterization

Photographs of the printed parts were captured using a Nikon D3200 camera with an 85 mm macro lens. The microscopic morphologies of the as-received CNT yarn, as-prepared CNT

yarn filament, and printed CNT yarn filament were investigated using optical microscopy (Leica, DM8000 M) and field emission-scanning electron microscopy (FE-SEM, Hitachi Model S-5200).

X-ray computed tomography (CT) data was acquired with a commercially available X-Tek (now Nikon Metrology) microfocus X-Ray Computed Tomography system, capable of resolving details down to 5 microns. X-ray source settings used during data acquisition were 160 kV operating voltage, 47 μA tube current, and 0.5 mm copper filter. Samples were mounted vertically between the source and detector, and radiographs collected at increments of approximately 0.11 degrees as the sample was rotated the full 360 degrees about its smallest dimension. Three-dimensional reconstructions of the collected radiographs produced volume data from which the cross sectional data in this study were extracted.

2.4 Mechanical testing

Room temperature tensile responses of the printed CNT yarn specimens were determined using a MTS-858 test frame equipped with a laser extensometer. The test specimen size and geometry were based on ASTM D638 (standard test method for tensile properties of plastic sheeting) and D1708 (standard test method for tensile properties of plastics by use of microtensile specimens) standards. The gage length and crosshead speed were 20 mm and 0.5 mm/min, respectively. At least three specimens, made under each print condition, were tested to determine tensile strength and modulus. The mechanical test data were normalized by the linear density of the specimen, which was determined by measuring the length and weight of the specimen to eliminate errors from the measurement of thickness and width of the specimen. The Young's modulus was calculated by linear regression at the slope between 100 and 200 MPa/(g/cm^3) in the specific stress vs. tensile strain curves, except for the data from neat Ultem®, where the slope from the initial, linear region of the stress-strain curve was used.

2.5 Electrical characterization

Four probe electrical conductivity measurements of the printed specimens were made using a Keithley 2400 current source and a Keithley 2000 DMM. Silver paint (Ted Pella Pelco® Colloidal Silver Paste, Product No. 16032) was used to attach the exposed CNT yarn ends to the measurement electrodes. Infrared thermographs were captured using a VT02 Visual IR Thermometer (Fluke Corporation). Piezoresistive data was acquired by metallizing the exposed ends of the CNT yarn in the printed part with Dupont 5000 silver ink. The CNT yarn ends were then connected through a terminal block to a Lakeshore Model 370 AC Resistance Bridge equipped with a Model 3708 pre-amplifier. The sample was placed on a custom-made 3 point bending fixture with 19 mm spacing between the outer contact points. Resistance measurements were captured at an acquisition frequency of approximately 0.45 Hz while a 50 N load was cyclically applied to and removed from the 3-point bending fixture.

3. Results and Discussion

3.1 CNT yarn filaments

Figure 1a shows a spool of printable CNT yarn filament. The average diameter of the filaments containing 10-30 % resin by weight was around 350 μm. The optical microscopy image of the CNT yarn filament in Fig. 1b shows that the CNT yarn is encapsulated with Ultem® resin. Scanning electron microscopy (SEM) reveals resin wet out of the interbundle spaces (Fig. 1c). The pristine CNT yarn (Fig. 1d) was uniformly coated with Ultem® 1010. No resin rich surfaces were observed.

3.2 CNT yarn filament printing and cutting

To demonstrate the placement and printing characteristics of CNT yarn filament, single filament traces were laid down. The CNT yarn filament was pushed into the substrate by the nozzle and held for ~1 s at strategic locations along the tool path to improve interfacial adhesion between the CNT yarn filament and the substrate. This “selective compaction”

(hereinafter selective compaction) method anchors the filament ahead of a long pass across the printing surface. The process worked well for printing of conductive traces quickly and in areas where robust adhesion was not required. A "continuous compaction" (hereinafter continuous compaction) method was used for areas where structural reinforcement was desired. In this process, the filament is pushed into the substrate at regular intervals over the entire CNT yarn filament trace during initial filament deposition. Heat is then reapplied during subsequent passes. For both methods, the accuracy of the print was maintained without requiring external intervention like clamps or adhesives to secure the CNT yarn filament prior to printing. These processes, along with the inherent high compliance of the CNT yarn, allowed the filament to be printed with high precision.

Figures 2a-c demonstrate the characteristics of the CNT yarn filament that make it a desirable feedstock for multifunctional parts. Tightly spaced, parallel filament lines can be printed to create parts with high concentrations of CNTs. The line spacings (from the center of one filament to that of the next) are 350 μm apart in Fig. 2a and 1 mm apart in Fig. 2b. This is a consequence of the tight turning radius (half the width of the yarn) that can be maintained by allowing the yarn to reorient itself over the course of the turn. There are no gaps visible between uniaxial line traces of the part shown in Fig. 2a. This is evidenced by the magnified printed CNT yarn filaments shown in Fig. 2c. In this figure, the ability to print continuous CNT yarn filaments having tight radii can also be seen. Deposition of multiple layers of the CNT yarn filament was also demonstrated. Figures. 2e and f show a 3D structure built with 28 layers of CNT yarn filament.

Increased versatility in the printing process can be achieved by integrating the ability to cut the CNT yarn filament at the deposition point when needed. Laser cutting and resistive (Joule) heating were explored for in-situ cutting of the CNT yarn filament. A 5W, 1570 nm diode laser (SemiNex Corp. 15P-110 Fiber Coupled Laser) was shown to be capable of

cutting the CNT yarn filament when tightly focused onto a spot on the filament. However, resistive heating provided a simpler, less expensive, quick, and controllable way to cut the CNT yarn filament on demand. Figure 3 shows the current and voltage vs. time curve for a typical cutting cycle at a power supply setting of 24 V and 3A. As voltage is applied, the current rises to a maximum in less than 200 ms, holds for ~300 ms and then drops to zero as the circuit is broken upon separation of the filament, allowing the measured voltage to rise to the set value for the now open circuit. The rise and fall in the current or the rise in the voltage can be used as a means to verify that the cutting was successful.

3.3 Imaging of 3D printed part

Figure 4a shows a printed sample illustrating the designations used to label images from X-ray CT. Fig. 4b shows the CT image of a sample printed using the selective compaction method. The image reveals microstructure characterized by large voids and a lack of Ultem® bridging between the yarns. This is the result of the shorter duration that the yarn is under heat and pressure when the selective compaction method is employed. In contrast, Figs. 4c and d show that the samples printed using continuous compaction have dense packing of the CNT yarn, indicating good adhesion between the filaments, as well as between the CNT yarn filament and the Ultem® substrate. To further characterize the effects of compaction, Fig. 4e shows a CT scan cross section aligned in the fiber direction for a one-layer specimen prepared using the selective compaction method. Areas of the sample that experienced compaction show dense packing of the CNT yarn, indicating good bonding between the printed yarn and the substrate, whereas areas where the yarn was pulled quickly across the surface show visible gaps between the yarn and the substrate.

3.4 Mechanical testing of 3D printed part

Mechanical test specimens of the CNT yarn filament were printed using both the selective and continuous compaction methods. Flat, 50 mm x 5.6 mm, specimens were printed with

the CNT yarn filament in a uni-directional layup pattern of one to three layers on a 127 μm thick Ultem® substrate. The nozzle height was not adjusted between layers, resulting in an increase in the compaction force with each additional layer. The Ultem® substrate remained adhered to the specimen during testing. The CNT content of the specimens is 27.8 ± 1.6% for the one-layer specimen and 42.3 ± 1.2% for the two-layer specimen.

Figure 5a shows typical stress strain curves for the specimens tested. The mechanical properties summarized in Fig. 5b show the effect of the two printing methods on mechanical performance. Continuous compaction produced specimens with higher mechanical performance and tighter tolerances than those from selective compaction, as evidenced by the smaller error bars. The addition of CNT reinforcement yielded a specific tensile strength of 317 MPa/(g/cm^3), and specific modulus of 19.5 GPa/(g/cm^3). These constitute a 287% improvement in the specific strength and 1850% increase in the specific modulus over the neat Ultem® sheet (measured specific strength and specific modulus 82 MPa/(g/cm^3) and 1.0 GPa/(g/cm^3) respectively as shown in Fig. 5a). Increasing the number of printed CNT yarn filament layers (and thus the CNT to polymer ratio) leads to an even higher increase in specific mechanical properties.

To further demonstrate embedding multifunctional and usable CNT based elements deep in a part, specimens were prepared using a dual nozzle printer. First, neat Ultem® was laid down on the print bed. Then, a single layer of CNT yarn filament was laid down using the selective compaction method and capped with layers of Ultem®. Dog-bone shaped tensile specimens were cut from these coupons and tested according ASTM D638 standard. These specimens have a higher resin to CNT content than the parts previously discussed and exhibit similar failure characteristics as the specimens printed using the selective compaction method. In spite of the low CNT content, the strength of the specimens increased from 89 ± 7 MPa (printed Ultem®) to 112 ± 4 MPa (4.7 wt.% CNT yarn reinforced Ultem®) (Fig. 5c). This

demonstrates the ability to print functional components without degrading structural performance of the part when the desired functionality does not require enhanced structural performance afforded by higher CNT yarn content.

3.5 Electrical characterization

The electrical properties of the printed specimens were tested using the 4-probe method.

Figure 6a shows the current-voltage (I-V) curves for the printed specimens with single conductive CNT yarn traces embedded deep in the specimen. These resin rich samples were printed as described for the sample shown in Fig 2b. The spacings between the CNT yarn filament lines in the specimens are 350 μm and 1 mm. The specimens were printed with equal lengths of CNT yarn filament. The plots show the I-V curves as current was raised from 0 A to 0.5 A before returning to 0 A.

Infrared (IR) thermographs of the specimens at 0 and 0.5 A are shown in Fig. 6a. Below 0.2 A, the I-V curves are linear. As Joule heating of the CNT yarn filament occurred, an increase in resistance led to a change in the I-V slope. At 5 watts of input power, the specimen temperature rose above 100 °C. The difference in cooling and heating rates led to some hysteresis upon the return of the current to zero. The properties returned to the as-printed state in subsequent low current sweeps. The resistance of the specimen with the 350 μm spacing is less than that for the one with the 1 mm spacing (11 and 16 Ω, respectively). This suggests that a few current carrying bridges exist between the traces in the specimen with the 350 μm spacing. However, even at this close spacing not all the paths are bridged. This is shown by the resistance being significantly higher than it would be if all CNT yarns were parallel (~ 2 Ω). The polymer coating that binds the filaments also acts as an insulator between them.

Embedded CNT yarn remains sufficiently conductive to act as an individual signal carrying path for powering a 1W lamp whether it is laid down using the selective compaction method

as in Figure 6b or as a flexible three layer structural reinforcement specimen built using continuous compaction as shown in Figure 6c. The continuously compacted specimen was electrically conductive in all directions (indicating that the compaction breaks the thin insulating barrier between the filaments). This enables application as a lightweight replacement to aluminum grounding plates, while the selectively compacted and insulated traces provide point-to-point signal routing.

Figure 6d shows the electrical response of a printed specimen as a 50 N load is applied to and removed from the specimen. A single trace of CNT yarn was used to form the sensing element. The as-printed CNT sensor shows a measurable and repeatable strain sensing response to loading and unloading. The multifunctionality of CNT yarn enables the printing of parts with embedded load sensitive paths that can be employed in applications such as adaptive structures and structural health monitoring.

As a further demonstration of the potential that CNT yarns and FFF provide to fabricate complex multifunctional parts, Fig. 7 shows a quadcopter printed with the CNT yarn filament as the mechanical reinforcement and current carrying conductor. Figure 7a shows the as-printed quadcopter structure with free ends of the CNT yarns that can be attached to other components. Figure 7b shows the fully assembled quadcopter with the rotors in motion as a result of current flowing through the embedded CNT yarns.

4. Summary and conclusions

Multifunctionality in a 3D printed part was demonstrated by utilizing CNT yarn filament and a thermoplastic polymer. Developments undertaken to permit FFF of Ultem® and CNT yarn filaments on an open-source printer were described. Approaches to overcome challenges associated with printing continuously reinforced components that were presented here include: a. development of a printable CNT yarn filament with a high performance polymer

matrix, b. development of the printing method yielding accurately placed, sufficiently adhered CNT yarn filament so measureable improvements in mechanical properties confirm structural reinforcement c. a simple cutting mechanism that permitted the termination of CNT yarn filament as needed at the point of deposition and automated initiation of the next print step. Successful implementation of the above methods on an inexpensive open-source printer was confirmed by determining the performance characteristics of the printed parts. Components were evaluated to demonstrate the mechanical property enhancement afforded by reinforcing Ultem® with CNT yarn and the added functionalities enabled by this structural reinforcement due to its electrical properties. Retention of the electrical conductivity in the CNT yarn filament allowed electrical components (wiring, heating elements and strain sensors) to be built directly into the structure of the 3D printed parts. Since CNT yarns are strong, electrically conductive, and highly flexible, strain gauges embedded into a part can act in both structural reinforcement and sensing capacities. The printed quadcopter showcases the potential to fabricate multifunctional, tailored components that take advantage of the suite of properties offered by CNT yarns.

Results presented here illustrate the potential for using CNT yarn to impart a variety of functions. Feedstocks with fillers that include continuous and chopped carbon fiber, Kevlar, conductive silver or low concentrations of graphene or CNTs are currently available, but do not provide the versatility demonstrated here with CNT yarns. This new approach reduces the number of interfacial challenges that can result from using multiple material types to attain the results shown here.

Received: ((will be filled in by the editorial staff))
Revised: ((will be filled in by the editorial staff))
Published online: ((will be filled in by the editorial staff))

[1] M. S. Dresselhaus, G. Dresselhaus, R. Saito, Physics of carbon nanotubes, in: M. Endo, S. Iijima, M. S. Dresselhaus (Eds.), Carbon Nanotubes, Elsevier, New York, 1996, pp. 27-36.

[2] S. Iijima, Helical microtubules of graphitic carbon, Nature 354 (1991) 56-58.

[3] N. A. Koratkar, B. Wei, P. M. Ajayan, Multifunctional structural reinforcement featuring carbon nanotube films, Compos. Sci. and Technol. 63 (2003)1525-1531.

[4] K. R. Atkinson, S. C. Hawkins, C. Huynh, C. Skourtis, J. Dai, M. Zhang, S. Fang, A. A. Zakhidov, S. B. Lee, A. E. Aliev, C. D. Williams, R. H. Baughman, Multifunctional carbon nanotube yarns and transparent sheets: fabrication, properties, and applications, Phys. B 394 (2007) 339-343.

[5] J. Qiu, C. Zhang, B. Wang, R. Liang, Carbon nanotube integrated multifunctional multiscale composites, Nanotechnology 18 (2007) 275708-11.

[6] M. Kaempgen, M. Lebert, N. Nicoloso, S. Roth, Multifunctional carbon nanotube networks for fuel cells, Appl. Phys. Lett. 92 (2008) 094103.

[7] C. Park, Z. Ounaies, K. A. Watson, R. E. Crooks, J. Smith, Jr., S. E. Lowther, J. W. Connell, E. J. Siochi, J. S. Harrison, T. L. St. Clair, Dispersion of single wall carbon nanotubes by in situ polymerization under sonication, Chem. Phys. Lett. 364 (2002) 303-308.

[8] E. T. Thostenson, T-W. Chou, Processing-structure-multi-functional property relationship in carbon nanotube/epoxy composites, Carbon 44 (2006) 3022-3029.

[9] P-C. Ma, N. A. Siddiqui, G. Marom, J-K. Kim, Dispersion and functionalization of carbon nanotubes for polymer-based nanocomposites: A review, Composites Part A 41 (2010) 1345-1367.

[10] M. F. L. De Volder, S. H. Tawfick, R. H. Baughman, A. J. Hart, Carbon nanotubes: present and future commercial applications, Science 339 (2013) 535-539.

[11] M. Guarrera, Soft Armor: Less Weight, More Comfort, http://www.nanocomptech.com/blog, April 17 (2014).

[12] Q. Cheng, J. Bao, J. G. Park, Z. Liang, C. Zhang, B. Wang, High mechanical performance composite conductor: multi-walled carbon nanotube sheet/bismaleimide nanocomposites, Adv. Funct. Mater. 19 (2009) 3219-3225.

[13] Q. Cheng, B. Wang, C. Zhang, Z. Liang, Functionalized carbon nanotube sheet/bismaleimide nanocomposites: mechanical and electrical performance beyond carbon fiber composites, Small 6 (2010) 763-767.

[14] J.-W. Kim, E. J. Siochi, J. Carpena-Núñez, K. E. Wise, J. W. Connell, Y. Lin, R. A. Wincheski, Polyaniline/carbon nanotube sheet nanocomposites: fabrication and characterization, ACS Appl. Mater. Interfaces 5 (2013) 8597-8606.

[15] J.-W. Kim, G. Sauti, E. J. Siochi, J. G. Smith, R. A. Wincheski, R. J. Cano, J. W. Connell, K. E. Wise, Toward high performance thermoset/carbon nanotube sheet nanocomposites via resistive heating assisted infiltration and cure, ACS Appl. Mater. Interfaces 6 (2014) 18832-18843.

[16] R. S. Downes, S. Wang, D. Haldane, A. Moench, R. Liang, Strain-induced alignment mechanisms of carbon nanotube networks, Adv. Eng. Mater. 17 (2015) 349-358.

[17] J.-W. Kim, G. Sauti, R. J. Cano, R. A. Wincheski, J. G. Ratcliffe, M. Czabaj, N. W. Gardner, E. J. Siochi, Assessment of carbon nanotube yarns as reinforcement for composite overwrapped pressure vessels, Composites Part A 84 (2016) 256-265.

[18] S. Harvey, Carbon as conductor: a pragmatic view, Proceedings of the 61st IWCS Conference (2013) 558-562.

[19] N. Behabtu, C. C. Young, D. E. Tsentalovich, O. Kleinerman, X. Wang, A. W. K. Ma, E. A. Bengio, R. F. ter Waarbeek, J. J. de Jong, R. E. Hoogerwerf, S. B. Fairchild, J. B. Ferguson, B. Maruyama, J. Kono, Y. Talmon, Y. Cohen, M. J. Otto, M. Pasquali, Strong,

light, multifunctional fibers of carbon nanotubes with ultrahigh conductivity, Science 339 (2013) 182-186.

[20] S. S. Crump, Apparatus and method for creating three-dimensional objects, US Patent 5,121,329 (1992).

[21] R. Jones, P. Haufe, E. Sells, P. Iravani, V. Olliver, C. Palmer, A. Bowyer, RepRap – the replicating rapid prototyper, Robotica 29 (2011) 177-191.

[22] C. Barnatt, 3D Printing, second ed., ExplainingTheFuture.com, 2014.

[23] B. M. Tymrak, M. Kreiger, J. M Pearce, Mechanical properties of components fabricated with open-source 3-D printers under realistic environmental conditions, Mater. Design 58 (2014) 242-246.

[24] E. García-Tuñon, S. Barg, J. Franco, R. Bell, S. Eslava, E. D'Elia, R. C. Maher, F. Guitian, E. Saiz, Printing in three dimensions with graphene, Adv. Mater. 27 (2015) 1688-1693.

[25] J. H. Kim, W. S. Chang, D. Kim, J. R. Tang, J. T. Han, G.-W. Lee, J. T. Kim, S. K. Seol, 3D printing of reduced graphene oxide nanowires, Adv. Mater. 27 (2015) 157-161.

[26] M. Nikzad, S. H. Masood, I. Sbarski, Thermo-mechanical properties of a highly filled polymeric composites for fused deposition modeling, Mater. Design 32 (2011) 3448-3456.

[27] S. B. Walker, J. A. Lewis, Reactive silver inks for patterning high-conductivity features at mild temperatures, J. Am. Chem. Soc. 134 (2012) 1419-1421.

[28] G. C. Pidcock, M. in het Panhuis, Extrusion printing of flexible electrically conducting carbon nanotube networks, Adv. Funct. Mater. 22 (2012) 4790-4800.

[29] D. Espalin, D. W. Muse, E. MacDonald, R. B. Wicker, 3D printing multifunctionality: structures with electronics, Int. J. Adv. Manuf. Technol. 72 (2014) 963-978.

[30] M. Namiki, M. Ueda, A. Todoroki, Y. Hirano, R. Matsuzaki, 3D printing of continuous fiber reinforced plastic, SAMPE Conf. Proc., Seattle, WA, June 2-15 (2014).

[31] G. T. Mark, A. S. Gozdz, Three dimensional printer with composite filament fabrication. U.S. Patent Application 14/575,180 (2014).

[32] J.-W. Kim, G. Sauti, E. J. Siochi, Resistive heating assisted infiltration and cure (RHAIC) for polymer/carbon nanotube structural composites. U.S. Patent Application 14/328,262 (2013).

[33] McMaster-Carr Ultem® data sheet, http://www.mcmaster.com/#8574kac/=122e0yd.

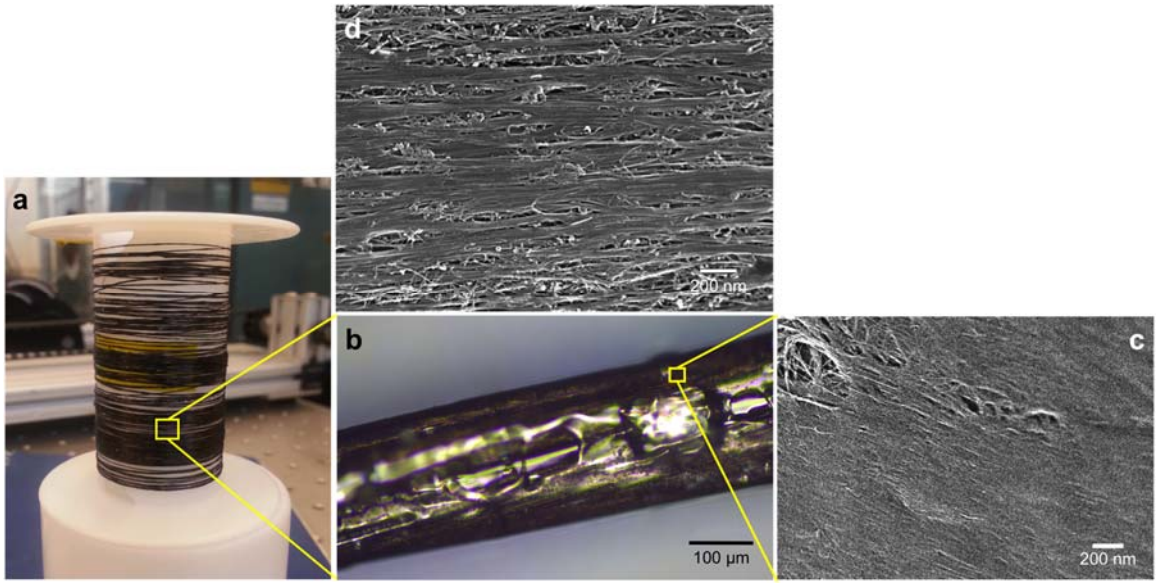

Figure 1. (a) Spool of CNT yarn filament prior to printing. (b) Optical microscopy image of individual CNT yarn filament. (c) SEM image of CNT yarn coated with Ultem® 1010. (d) SEM image of pristine CNT yarn.

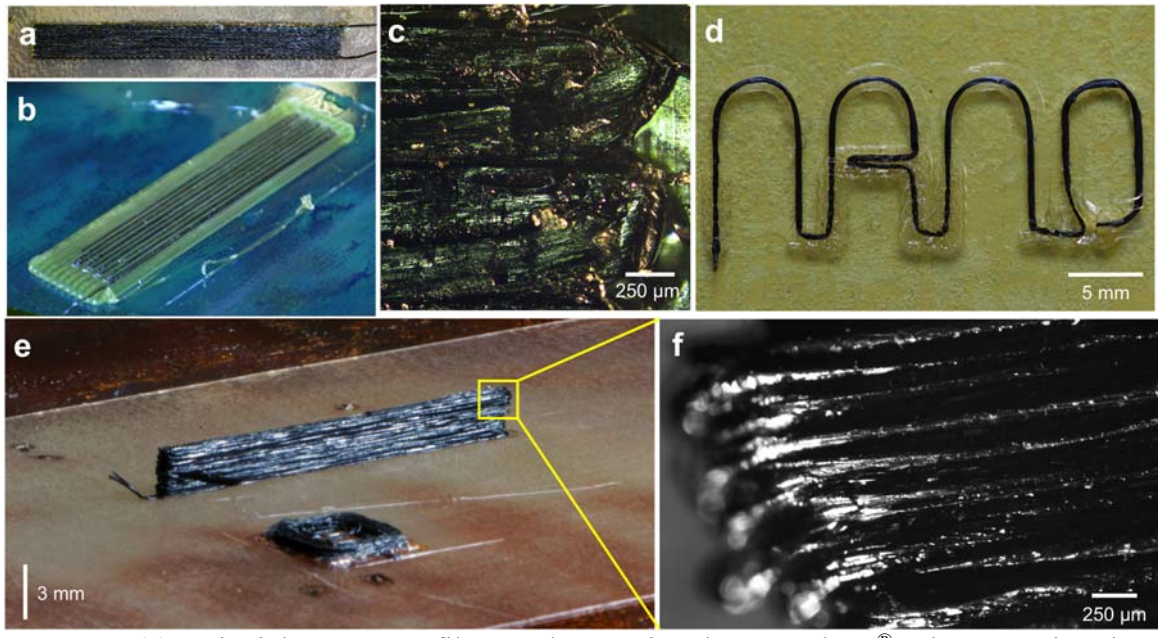

Figure 2. (a) Uniaxial CNT yarn filament layer printed on an Ultem® substrate using the continuous compaction method. The specimen measures 50 mm x 5.6 mm. (b) A resin rich specimen with an embedded electrical signal carrying CNT trace. (c) higher magnification of 2(a) showing the 180° turns possible with printed CNT yarn. (d) The letters "nAno" printed using a single CNT yarn filament showing 90°, 180°, and large radius turns. Individual letters are 10 mm by 5 mm. (e) Printed walls. Foreground: 10-layer square border. Background: 28-layer thin wall. Both objects contain ~86 wt.% CNT. (f) Close-up view of thin wall showing 12 individual layers of CNT yarn.

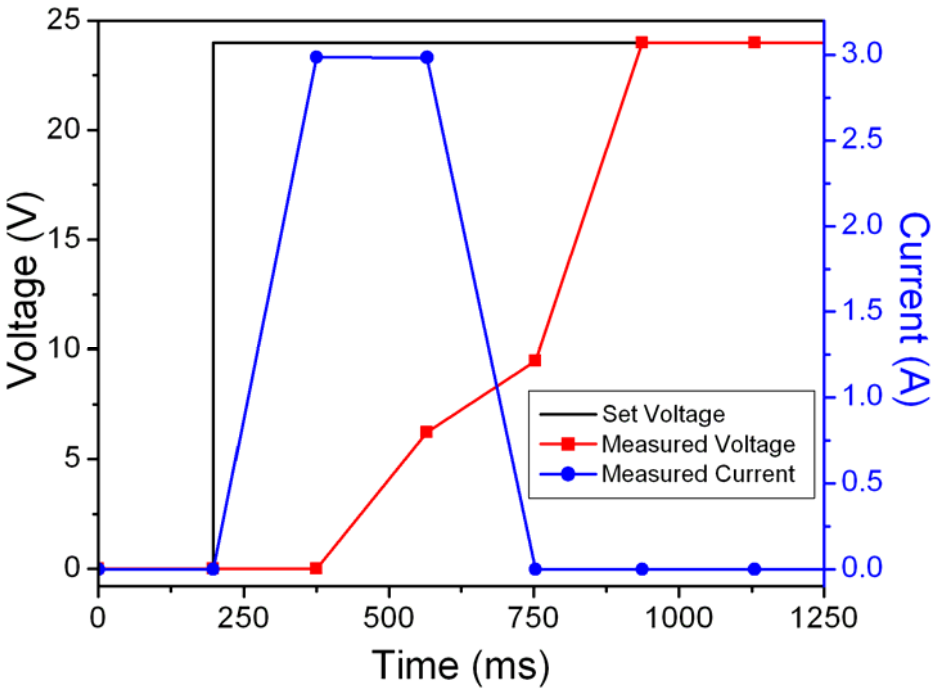

Figure 3. The voltage and current vs. time profile for a CNT yarn filament cut.

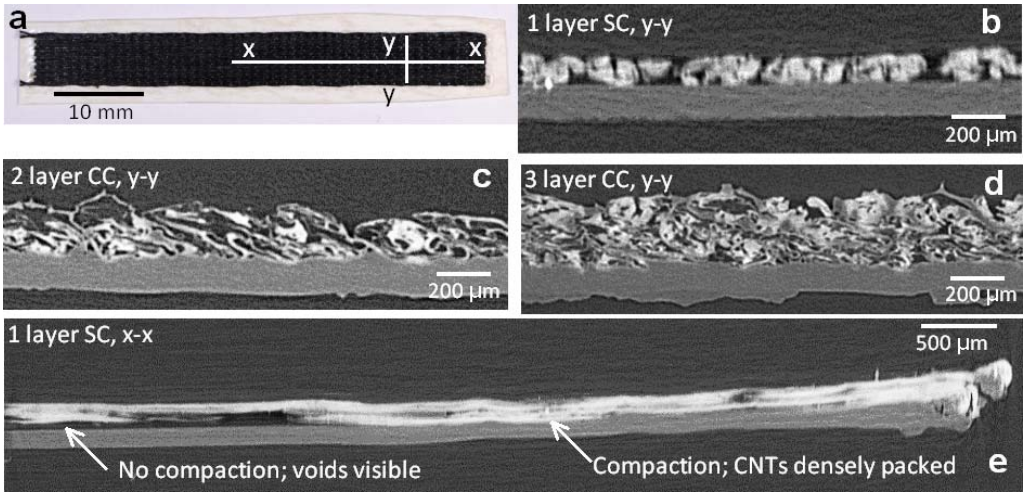

Figure 4. (a) Typical printed specimen with cross sections used for the Computer-aided tomography (CT) scans shown. (b-e) CT scans of printed specimens.

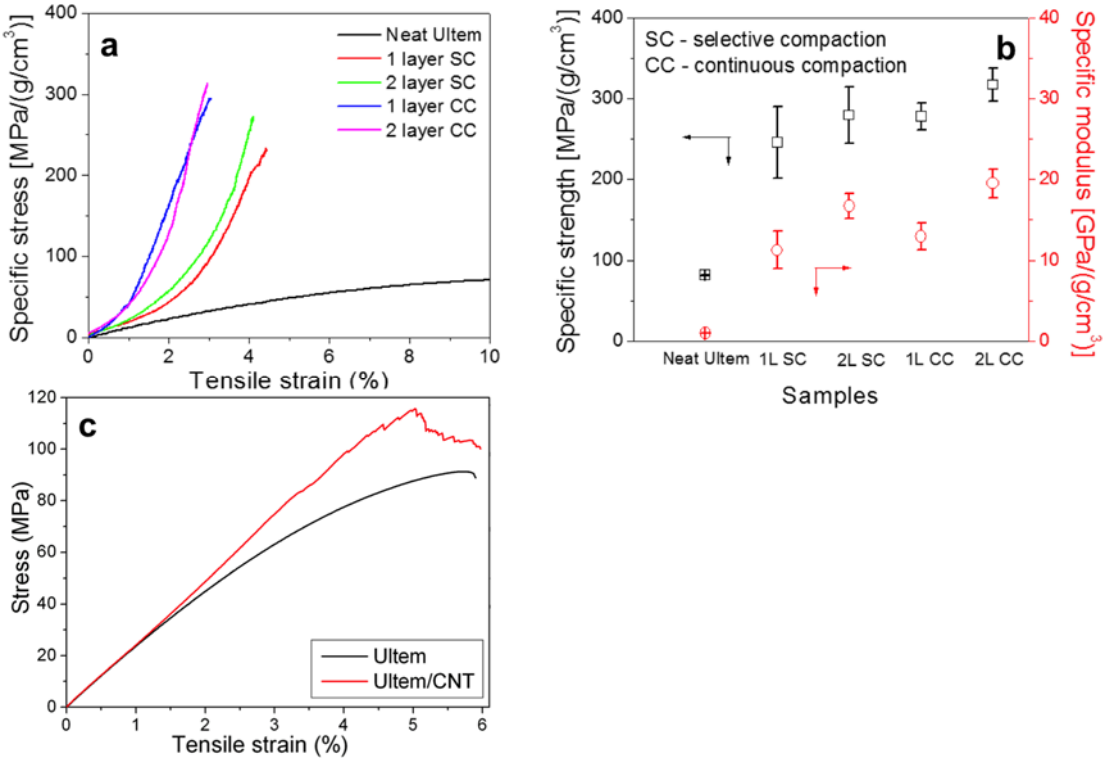

Figure 5. (a) Stress-strain curve showing one and two layer uniaxial CNT rich CNT yarn filament specimens printed using selective and continuous compaction. (b) Graph of the mechanical response of the printed specimen. (c) Tensile test data for resin rich specimens containing printed CNT yarn electrical current carrying traces.

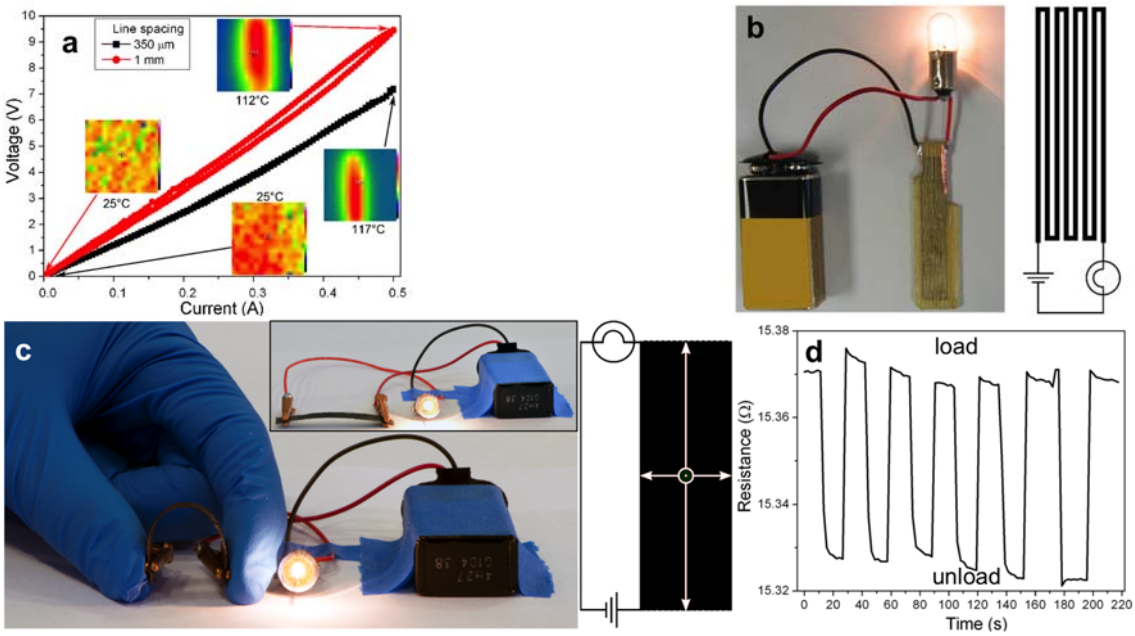

Figure 6. (a) I-V curves for CNT yarn traces printed with 1 mm and 350 μm spacing between the filament centers. The inserts show IR thermographs at zero and maximum current. (b) 1 W bulb powered through the specimen shown in Fig. 2b. (c) A 1-W bulb powered through a three layer CNT yarn specimen printed using continuous compaction. The main figure shows the specimen under a bending load while the inset shows it without loading. The circuit schematics in (b) and (c) show the current paths within the printed specimens. (d) Electrical response of a printed specimen to cyclical mechanical loading.

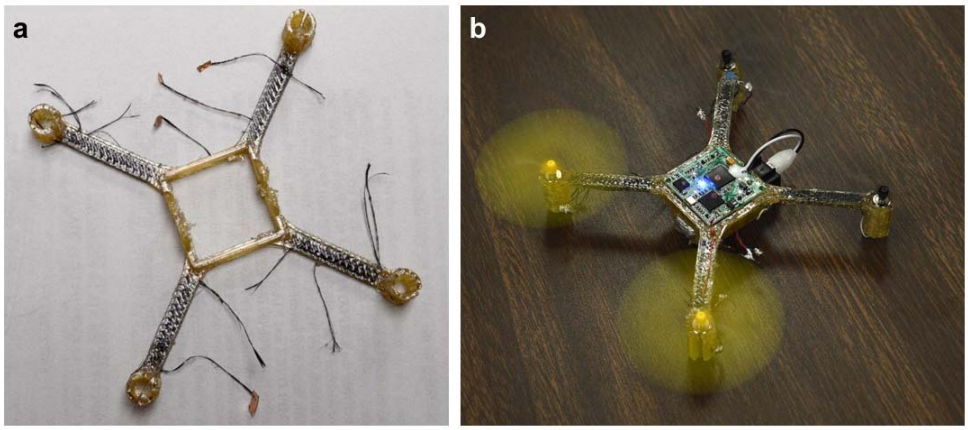

Figure 7. (a) A quadcopter frame printed using neat Ultem® and CNT yarn filaments. The frame measures 115 mm from tip to tip. (b) The fully assembled quadcopter with the motors powered via the CNT yarn that also functions as a mechanical reinforcement.